



Laboratory Investigation of Anisotropic Shrinkage of HLW Buffer Block: An Attempt Using Digital Image Correlation Method

Huyuan Zhang^{1,2(✉)}, Yu Tan¹, Dongjin He¹, and Gang Luo¹

¹ School of Civil Engineering and Mechanics, Lanzhou University,
Rd 222 South Tianshui, Lanzhou 730000, Gansu, China
zhanghuyuan@lzu.edu.cn

² Key Laboratory of Mechanics on Disaster and Environment in Western China
(Lanzhou University), Ministry of Education, Lanzhou 730000, China

Abstract. Anisotropic shrinkage of compacted bentonite blocks threatens the security of a buffer barrier in a geological disposal project for high-level radioactive wastes (HLW). In this investigation, fan-shaped buffer blocks on an industrial scale were compacted and exposed to an indoor environment to dry naturally. Digital image correlation (DIC) was used in an attempt to monitor the blocks' shrinkage deformation in a vertical (z) direction, and dial indicators were used to measure horizontal (r and θ) shrinkage for comparison. Before and after the blocks desiccation, pore size distributions were investigated by mercury intrusion porosimetry (MIP) to analyze the shrinkage behavior in the microstructure, and the micro-fissuring was investigated by X-ray computed tomography (CT) in terms of internal visual structure. The initial evaporation stage on the industrial scale and over compaction of the blocks was not detected. In horizontal directions, isotropic shrinkage strains were observed, which were lesser than 2%. Linear shrinkage strains decreased with the increase of the initial lengths of the measuring lines, indicating that block shrinkage is mainly concentrated on the external part, while the internal part shows poorer shrinkage ability. CT images showed that no obviously micro-fissuring was found in a block before drying it and MIP results demonstrated that both macrostructure and microstructure at a 5 cm depth slightly changed after block desiccation. Vertical shrinkage, monitored by DIC, exhibited a poorer ability compared to the horizontal direction, which had almost equal linear strains though its initial measuring lines lengths were shorter. In future research, more attention should be paid to the lateral shrinkage of buffer blocks.

Keywords: High-level radioactive waste (HLW) · Bentonite block
Desiccation · Anisotropy shrinkage · Digital image correlation (DIC)

1 Introduction

Deep geological disposal is widely accepted as a promising way to dispose of high-level radioactive wastes (HLW) in line with the development of nuclear science. In Chinese disposal project, compacted GMZ bentonite block can be used to build an

engineering barrier and its quality guarantees the security of the disposal project. Other countries, such as Spain [1], Czech Republic [2], and Sweden [3], have attached great significance to the buffer block research. If bentonite blocks were exposed to the atmosphere during its storage and transportation, they would dry and shrink due to the relatively higher compacted moisture content [4]. Therefore, in the construction of buffer barrier, blocks joints will widen in these shrunken blocks and the function of the barrier, such as hyposmosis, will be seriously damaged.

Research studies on the shrinkage of buffer blocks on an industrial scale are limited. SKB [4] reported the shrinkage of compacted bentonite specimens in a laboratory that were exposed to 35% relative ambient humidity. Different shrinkages between blocks and specimens may be found because of scale effects. Peron [5] focused on the desiccation of a paste-like, fine-grained soil, but such work conducted on paste-like specimens cannot replace the research of compacted blocks. Moreover, anisotropic shrinkage is enlarged by the blocks industrial scale. There is an urgency to guarantee the quality of buffer blocks in terms of shrinkage to participate with a plan for building a Chinese underground laboratory for HLW disposal in 2020.

Considering large-scale buffer blocks, there is a lack of accuracy in measuring their shrinkage strain by traditional equipment, such as a digital caliper. Since digital image correlation (DIC) was put forward [6, 7] to precisely measure the full-field strain, many researchers [8, 9] have made contributions to this technique being applied to engineering to measure concrete strains and cracks.

The purpose of this work is to investigate the anisotropic shrinkage of buffer blocks comprised bentonite and sand. These were compacted on an industrial scale and exposed in an indoor condition to monitor the desiccation shrinkage and moisture content. In a vertical direction, block shrinkage strain was measured by DIC, and the horizontal shrinkage strain was measured by dial indicators for comparison. Mercury intrusion porosimetry (MIP) and X-ray computed tomography (CT) were used to investigate the pore size distributions and visual fissures, respectively. Based on the test results, the three-direction (3D) shrinkage characteristics of buffer blocks are noted and now the priorities for further research on buffer block can be suggested.

2 Materials and Methods

2.1 Material Characterization

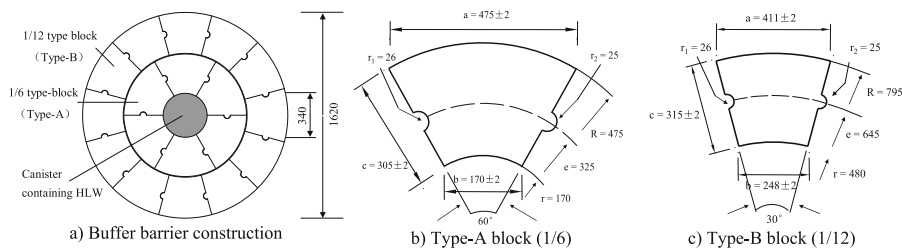
The GMZ bentonite used in this work was mined in Inner Mongolia, China. As reported, quartz sand was added to bentonite at a 7:3 mass ratio, which improves the buffer materials' properties, such as reinforcing thermal conductivity [10] without undermining the buffer's permeability [11] and swell property [12]. The quartz sands were obtained from Yongdeng, China. Material properties are summarized in Table 1.

2.2 Buffer Block Preparations

Until now, the construction of an engineering buffer has not been determined for China's HLW disposal. An idealized conception of a buffer barrier (Fig. 1), with patent

Table 1. Basic properties of bentonite and quart sand used.

GMZ bentonite					Sand		
Particle diameter	Air dry moisture contents	Liquid limit	Plastic limit	Specific gravity	Particle diameter	Silica contents	Specific gravity
Main < 2 (μm)	9 (%)	160.7 (%)	30.65 (%)	2.70 (g/cm^3)	0.2–2.0 (mm)	>99 (%)	2.65 (g/cm^3)

**Fig. 1.** The conception of constructing the compacted blocks together (unit: mm)

authorization, was put forward following other in-country projects [1, 2, 13]. Bentonite-sand mixtures were compacted to prepare Type-B blocks at about 10 cm height by using a uniaxial compressor in this work. Before the compaction, bentonite powders and quartz sands with a 7:3 mass ratio were uniformly mixed to obtain 18% moisture contents after spraying water and were then sealed for preservation in plastic bags for 48 h to reach a uniformly humidifying. After compaction, blocks were sealed in plastic wraps for 1 month to uniformly humidify and stabilize the shape.

2.3 Desiccated Condition

As reported, the Beishan area in Gansu Province is a promising site for disposing of HLW in China [14]. In this setting, the local climate is a key factor for block shrinkage during transportation and storage. In this work, the blocks were desiccated at the relative humidity of the atmosphere of Lanzhou, where is the capital of Gansu Province. Test results have contributed to the quality control for these buffer blocks.

2.4 Shrinkage Strain Measurements

After correlating certain subsets of pixels in the reference image with their homologous ones in the deformation image [15, 16], DIC measures strain by catching special pixels created by speckles. In this work, white paint was spotted on a block vertical surface and then black points were added on these white spots to create speckles. By this method, not field strain but linear strain on a block was measured vertically by DIC. A quarter of the block was used to measure the strain (Fig. 2a). Another quarter of the block at the same ambient was used to record moisture content by interval weighing,

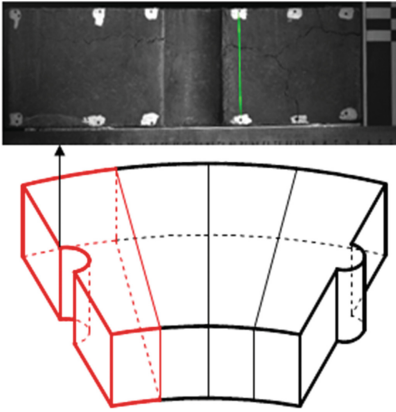
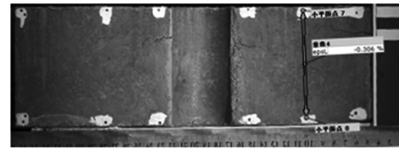
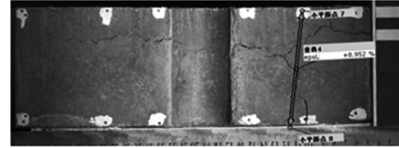


Fig. 2a. Block shrinkage monitor in vertical direction by DIC



Initial designed measuring line



Mistake occurred in measuring line

Fig. 2b. An example of a DIC mistake

measure the vertical height by a digital caliper (0.01 mm precision) for comparison. The height of the quarter block was the average value of six measuring lines to minimize a measuring error. In this work, the horizontal shrinkage strain of a buffer block (unpublished) is also presented as a comparison.

2.5 X-Ray CT Tests

X-ray CT is a non-invasive technique that can be used to visualize the interior of objects based on the attenuation of an electromagnetic wave. This technology has been widely used in geotechnique and soil science [17–19]. To observe the internal of the block apparently, the spatial resolution of the CT device is 24 LP/cm (i.e., 0.208 mm), the block is sawed into a cuboid segment of about $10 \times 10 \times 20$ cm in size.

3 Experimental Results

3.1 Evaporation Process

In this test, a quarter of a block and a whole block were dried at indoor condition at Lanzhou and their moisture contents were recorded by interval weighs as showed in Fig. 3. These two curves follow a similar variation trend, which decrement rates of moisture content gradually decrease as shown by the curves tending to horizontal. In general, the evaporation curve can be divided into an initial stage, a falling stage and a residual stage [20]. At the initial stage, the evaporation rate almost stays constant which is accompanied by a linear decrease of moisture content as time lapsed. At the falling stage, the water evaporation rate sharply decreases and then gradually becomes constant by turning into the residual stage. However, the initial stage was not observed in block evaporation as shown in Fig. 4. As reported, the falling evaporation rate is the

result of the evaporating interface transforming from the material surface to inside. Hierarchical evaporation occurs in buffer blocks due to their industrial scale, such as a block’s external part evaporating initially and its internal part evaporating later. The internal part, a large portion of an industrial scale block, exhibits falling evaporation for a long period in comparison to the external part’s evaporation. This phenomenon leads to trouble in detecting the short duration of the initial evaporation stage. Besides, moisture in an overly compaction block lacks connectivity, so its internal moisture is hard to transform in a timely way to the block surface to keep up a constant evaporate rate. This feature also contributes to the undetectability of the initial evaporation stage.

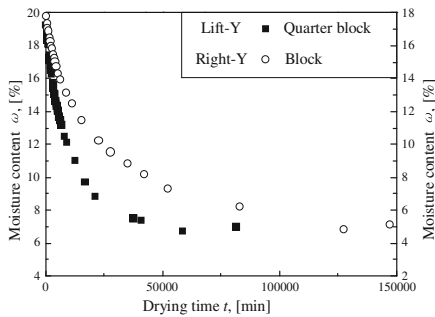


Fig. 3. Evolution of water content with time

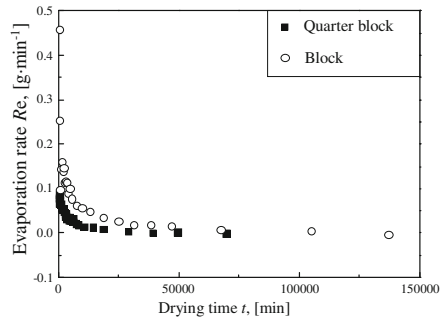


Fig. 4. Evolution of evaporation rate with time

3.2 Shrinkage Strain

According to preliminary research, isotropy horizontal shrinkages in r and θ directions were measured by a specially designed device equipped with 20 fixed dial indicators. Linear shrinkage strain in each direction takes the average value of 5 measuring lines by 10 fixed dial indicators, and the average initial length of measuring lines in r and θ direction is 315 mm and 336 mm, respectively.

In a vertical direction, speckles were painted to create 6 measuring lines to monitor block vertical shrinkage by DIC. However, these speckles were not always precisely recognized by DIC as shown in Fig. 2b. After carefully inspecting the analysis process, we determined only 1 measuring line combined 2 speckles in a vertical direction, and this was adopted for the analysis that showed no obvious mistake.

Vertical linear shrinkage strains as measured by both DIC and digital caliper were presented in Fig. 5, as well as strains in r and θ direction. Parallel blocks, used to measure vertical strain and horizontal strain, respectively, were slightly different in the initial moisture due to imprecise block preparation. For a better comparison, top-X axis was used to make strain curves start at the same point. In Fig. 5, vertical strain measured by DIC presents almost the same variations with a horizontal direction at initial shrinkage. And the result of vertical shrinkage strain measured by digital caliper is similar to DIC results, but it is indeterminate because the whole shrinkage in a vertical direction is only about 2 mm. The final horizontal strains are less than 2%.

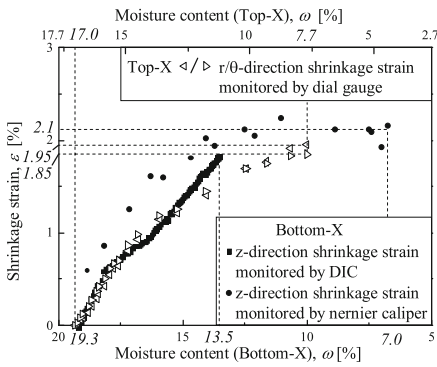


Fig. 5. Shrinkage strain curves in $r/\theta/z$ direction

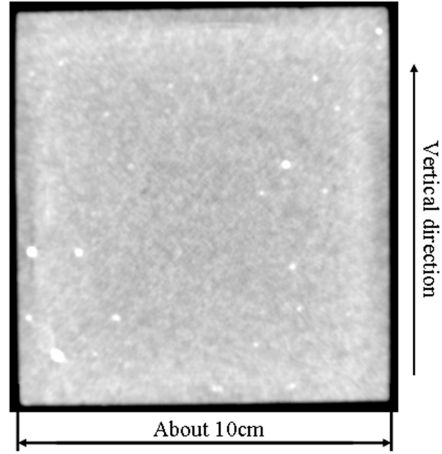


Fig. 6. An example of CT image for a part of block with 18% moisture content

4 Discussions

In the horizontal shrinkage of a block, linear strains decreased with an increase of the initial length of measuring lines. While shrinkage variations of each measuring lines with a different initial length were nearly identical. It is conjectured that block shrinkage strain is mainly concentrated on the external part and the internal part shows poor shrinkage ability.

In order to test this conjecture, pore distributions of block internal parts before and after block desiccation were investigated by MIP tests. A dried specimen was taken at 5 cm depths under a dried block top face and side face, and an un-dried parallel block was used to obtain an un-dry specimen. Specimens should be freeze-dried to keep their porous characteristics without any seriously shrinkage during moisture desorption. Comparing the cumulative pore volume obtained from the un-dried and dried block, Fig. 7a shows that the intruded mercury volume of a block after drying is remarkable higher than for a block before drying. However, the mine difference of intruded mercury volume cumulated at the initial of MIP tests, and the peaks of pore size density curves of blocks before and after drying were similar (as showed in Fig. 7b) compared to Hashmei [21] results. According to Lloret [22], pore size around $0.06 \mu\text{m}$ and $6 \mu\text{m}$ can be recognized as a microstructure and a macrostructure respectively, and pore sizes larger than $200 \mu\text{m}$ (Fig. 7b) are considered as visual structures. It can be distinguished that the block's macrostructure is basically unchanged and its microstructure has slightly accumulated after desiccation, while the visual structure remarkably increased. Visual structure detected by a CT scan uses a cuboid segment taken from an undried block. No visual fissures were detected by CT images (Fig. 6) as the MIP tests have shown. The visual structure in un-dried block tested by MIP is considered as the result

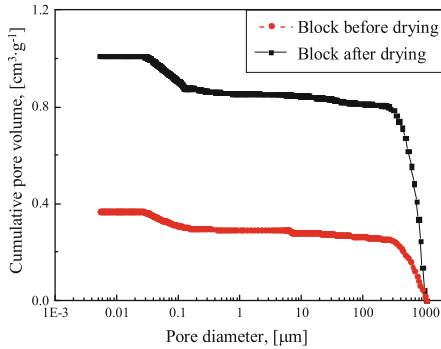


Fig. 7a. Cumulative pore volume curves

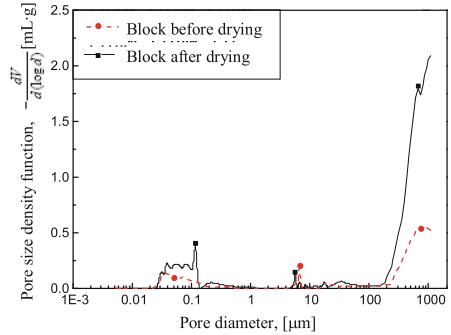


Fig. 7b. Differential pore volume curves

of a disturbance during sample preparation. The visual structure of dried blocks cannot change seriously (Fig. 7b) given the circumstances that the macrostructure and the microstructure were not changed remarkably after drying. So a conclusion can be drawn that shrinkage is apparently not detected by MIP and CT tests at a 5 cm depth of a block, which corresponds to our conjecture based on the results of the horizontal strain.

Figure 5 shows that linear shrinkage strain in a vertical direction corresponds to the strain in a horizontal direction. However, the initial length of the vertical measuring line, around 10.5 cm, is shorter than the average horizontal lengths. Even take an unvaporized bottom into consideration, measuring line initial length in a vertical direction is still shorter than half a length of horizontal measuring lines. As remarkable shrinkage was not detected below the 5 cm depth of the block, shrinkage strain should increase with the decrease of measuring line's initial length when the shrinkage ability keeps constant. The correspondence of vertical and horizontal shrinkage means that with a shorter initial length, the block has poorer shrinkage ability. As a result, poorer shrinkage ability in a vertical direction corresponds to the situation that compaction was exerted in a vertical direction, and uniaxial compaction leading to well orientation of smectite platelets [23] may restrain the vertical shrinkage of blocks.

5 Conclusions

- (1) The initial stage was not detected in block evaporation and so the constant evaporation ratio did not keep periods in comparison to the longer duration of the falling and residual stages. Block's distinguishing features, industrial scale, and over-compaction contributes to this result of bringing about hierarchical evaporation from the block's external part to its internal part and restricting the connectivity of the block moisture.
- (2) 5 cm depth of blocks did not remarkably shrink according to similar pore distributions before and after desiccation as tested by MIP under the circumstance that no obvious visual fissures were detected by CT scan in an un-dried block.

- (3) Vertical shrinkage ability presented by DIC was poorer than in a horizontal direction because vertical strain was similar to horizontal direction and the initial lengths of the measuring lines were obviously shorter. Vertical compaction is partly responsible for the poorer shrinkage ability. The final shrinkage strain of buffer is about 2%, and much attention should be paid to lateral shrinkage of buffer block.

Acknowledgments. The authors are grateful to the National Nature Science Foundation of China (41672261) and Fundamental Research Funds for the Central Universities (Izujbky-2017-ct02) for their financial support.

References

1. Martin PL, Barcala JM (2005) Large scale buffer material test: mock-up experiment at CIEMAT. *Eng Geol* 81(3):298–316
2. Pacovský J, Svoboda J, Zapletal L (2007) Saturation development in the bentonite barrier of the Mock-Up-CZ geotechnical experiment. *Phys Chem Earth* 32(8–14):767–779
3. Svensk K (2010) Design, production and initial state of the buffer. TR-10-15, SKB, Swedish
4. Torbjorn S, ULF Nilsson, L Andersson (2016) Investigation of parameters influencing bentonite block quality. P-16-06, SKB, Swedish
5. Peron H, Hueckel T, Laloui L et al (2009) Fundamentals of desiccation cracking of fine-grained soils: experimental characterisation and mechanisms identification. *Can Geotech J* 46(10):1177–1201
6. Yamaguchi I (1981) A laser-speckle strain gauge. *J Phys E Sci Instrum* 14(11):1270–1273
7. Peters WH, Ranson WF (1982) Digital imaging techniques in experimental stress analysis. *Opt Eng* 21(3):213427
8. Corr D, Accardi M, Graham-Brady L et al (2007) Digital image correlation analysis of interfacial debonding properties and fracture behavior in concrete. *Eng Fract Mech* 74(1–2):109–121
9. Helm JD (2008) Digital image correlation for specimens with multiple growing cracks. *Exp Mech* 48(6):753–762
10. Chen H, Zhang HY, Guo YQ et al (2014) Measurement and prediction of thermal properties of bentonite-sand mixture as buffer backfilling materials for high level radioactive waste. *Chin J Rock Mech Eng* S2:4312–4320
11. Zhou L, Zhang HY, Yan M et al (2013) Laboratory determination of migration of Eu(III) in compacted bentonite–sand mixtures as buffer/backfill material for high-level waste disposal. *Appl Radiat Isot* 82:139–144
12. Cui SL, Zhang HY, Zhang M (2012) Swelling characteristics of compacted GMZ bentonite–sand mixtures as a buffer/backfill material in China. *Eng Geol* 141:65–73
13. Villar MV, Iglesias RJ, Gutierrez AC et al (2018) Hydraulic and mechanical properties of compacted bentonite after 18 years in barrier conditions. *Appl Clay Sci* 160:49–57
14. Zhao XG, Wang J, Chen F et al (2016) Experimental investigations on the thermal conductivity characteristics of Beishan granitic rocks for China’s HLW disposal. *Tectonophysics* 683:124–137
15. Wang LL, Zhang GQ, Hallais S et al (2017) Swelling of shales: a multiscale experimental investigation. *Energy Fuel* 31(10):10442–10451

16. Wang LL, Tang CS, Shi B et al (2018) Nucleation and propagation mechanisms of soil desiccation cracks. *Eng Geol* 238:27–35
17. Raynaud S, Ngan-Tillard D, Desrues J et al (2008) Brittle-to-ductile transition in Beaucaire marl from triaxial tests under the CT-scanner. *Int J Rock Mech Min Sci* 45(5):653–671
18. Helliwell JR, Sturrock CJ, Grayling KM et al (2013) Applications of X-ray computed tomography for examining biophysical interactions and structural development in soil systems: a review. *Eur J Soil Sci* 64(3):279–297
19. Soto-Gómez D, Pérez-Rodríguez P, Vázquez-Juiz L et al (2018) Linking pore network characteristics extracted from CT images to the transport of solute and colloid tracers in soils under different tillage managements. *Soil Tillage Res* 177:145–154
20. Zhang Y, Ye WM, Chen B et al (2016) Desiccation of NaCl-contaminated soil of earthen heritages in the Site of Yar City, northwest China. *Appl Clay Sci* 124:1–10
21. Hashemi MA, Massart TJ, Salager S et al (2015) Pore scale characterization of lime-treated sand–bentonite mixtures. *Appl Clay Sci* 111:50–60
22. Lloret MA, Villar MV, Sanchez M et al (2003) Mechanical behaviour of heavily compacted bentonite under high suction changes. *Geotechnique* 53(1):27–40
23. Lee JO, Choi H, Lee JY (2016) Thermal conductivity of compacted bentonite as a buffer material for a high-level radioactive waste repository. *Ann Nucl Energy* 94:848–855